

Genetic Immunization Using Nanoparticles Engineered from Microemulsion Precursors

Zhengrong Cui¹ and Russell J. Mumper^{1,2}

Received March 13, 2002; accepted March 26, 2002

Purpose. Genetic immunization using “naked” plasmid DNA (pDNA) has been shown to elicit broad humoral and cellular immune responses. However, more versatile and perhaps cell-targeted delivery systems are needed. To this end, a novel process to engineer cationic nanoparticles coated with pDNA for genetic immunization was explored.

Methods. Cationic nanoparticles were engineered from warm oil-in-water microemulsion precursors composed of emulsifying wax as the oil phase and cetyltrimethylammonium bromide (CTAB) as the cationic surfactant. Plasmid DNA was coated on the surface of the cationic nanoparticles to produce pDNA-coated nanoparticles. An endosomolytic lipid and/or a dendritic cell-targeting ligand (mannan) were incorporated in or deposited on the nanoparticles to enhance the *in vitro* cell transfection efficiency and the *in vivo* immune responses after subcutaneous injection to Balb/C mice. The IgG titer to expressed β -galactosidase and the cytokine release from isolated splenocytes after stimulation were determined on 28 days.

Results. Cationic nanoparticles (around 100 nm) were engineered within minutes. The pDNA-coated nanoparticles were stable at 37°C over 30 min in selected biologic fluids. Transmission electron microscopy showed the nanoparticles were spherical. Plasmid DNA-coated nanoparticles, especially those with both an endosomolytic lipid and dendritic cell-targeting ligand, resulted in significant enhancement in both IgG titer (over 16-fold) and T-helper type-1 (Th1-type) cytokine release (up to 300% increase) over “naked” pDNA.

Conclusion. A novel method to engineer pDNA-coated nanoparticles for enhanced *in vitro* cell transfection and enhanced *in vivo* immune responses was reported.

KEY WORDS: plasmid DNA; mannan; pullulan; T-helper cell; β -galactosidase.

INTRODUCTION

Genetic immunization using either “naked” pDNA or pDNA-laden gold beads (gene gun) has gained considerable interest since the first demonstration of both protective immunity and cytotoxic T lymphocyte (CTL) responses in mice (1). The ability of pDNA-based vaccines to elicit both humoral and cellular immune responses is a key advantage over conventional subunit (protein) or whole-killed viral vaccines (2–4). Vaccines that generate cellular immunity mediated by the generation of CTL responses have been called the “the immunologist’s grail” (5). These vaccines may be of prime importance for protection from intracellular viral infections and/or as potential immunotherapies for cancer. Immunization with “naked” plasmid DNA has been found to induce

strong T-helper cell type-1 (Th1) immune responses as evidenced by the production of cytokines such as interleukin-2 (IL-2) and interferon- γ (IFN- γ) (6,7). In contrast, subunit, or protein-based, vaccines tend to induce T-helper cell type-2 (Th2) immune responses as evidenced by the generation of cytokines such as IL-4 and IL-10. Significantly, Th1 cells aid in the regulation of cellular immunity whereas Th2 cells aid in the production of antibodies. Improved immunization methods to enhance Th1-type immune responses in parallel with enhanced (neutralizing) antibody production are needed in the field.

Recent positive clinical data using the gene gun to administer submilligram amounts of pDNA into the skin epidermis has both validated this technology as a viable clinical vaccine modality and highlighted the rationale of targeting vaccines to antigen presenting cells residing in either the skin (Langerhan’s cells) or the draining lymph node (8). However, it is unclear whether or not this technology will become commercially viable because of potential scale-up and cost considerations. Several reports have demonstrated enhanced immune responses (cellular and humoral) using nanoparticles or microparticles (9–15). For example, Singh *et al.* (12) demonstrated both enhanced humoral and CTL responses in mice over “naked” plasmid DNA after intramuscular injection of pDNA-coated cationic poly(lactic acid-co-glycolic acid) (PLGA) microspheres having diameters from 300 nm to 30 μ m. They also reported an inverse correlation between the size of the microparticles and their elicited immune response, wherein the smallest particles (300 nm) led to the highest immune response (12).

In this article, we report a method to engineer smaller cationic nanoparticles from microemulsion precursors. The method is based on the spontaneous formation of warm microemulsions that can easily be used as a template to form cationic nanoparticles. This microemulsion precursor strategy has advantages because 1) all ingredients are potentially biocompatible; 2) the natural engineering process can easily be adapted to include many different excipients such as adjuvants, endosomolytic agents; 3) well-defined and uniform solid nanoparticles (<100 nm) may be reproducibly made without the use of expensive and/or damaging high-torque mechanical mixing, microfluidization, or homogenization; 4) no organic solvents are used during the manufacturing process; 5) very high entrapment efficiencies are achievable, especially for water-insoluble drugs; 6) the formed solid nanoparticles may have superior *in vivo* stability; and 7) cell-specific ligands can easily be incorporated into the nanoparticles (during or after the engineering process). The overall objective of these studies was to develop and characterize pDNA-coated nanoparticles and compare the humoral and Th1-type immune responses of pDNA-coated nanoparticles to those of “naked” pDNA after subcutaneous injection to mice.

MATERIALS AND METHODS

Materials

Plasmid DNA containing a CMV promoter β -galactosidase reporter gene (CMV- β -gal) and luciferase gene (CMV-Luc) were generous gifts from Valentis, Inc. (The Woodlands,

¹ Division of Pharmaceutical Sciences, College of Pharmacy, University of Kentucky, Lexington, Kentucky 40536-0082.

² To whom correspondence should be addressed. (e-mail: rjmump2@uky.edu)

Texas). Emulsifying wax was purchased from Spectrum Quality Products, Inc. (New Brunswick, New Jersey). Nonionic emulsifying wax is comprised of cetyl alcohol and polysorbate 60 in a molar ratio of about 20:1. Cetyltrimethylammonium bromide (CTAB), β -galactosidase, normal goat serum, and Sephadex G-75 were from Sigma Chemical Co. (St. Louis, Missouri). Phosphate-buffered saline (PBS)/Tween 20 buffer (20X) was obtained from Scytek Laboratories (Logan, Utah). Tetramethylbenzidine (TMB) Substrate Kit was from Pierce (Rockford, Illinois). Anti-mouse IgG peroxidase-linked species-specific F(ab')₂ fragment (from sheep) was purchased from Amersham Pharmacia Biotech Inc. (Piscataway, New Jersey). *N*-[2-(Cholesterylcarboxyamino)ethyl] carbamoylmethyl]mannan or pullulan (cholesterol-mannan or cholesterol-pullulan) were purchased from Dojindo Molecular Technologies, Inc. (Gaithersburg, Maryland). Mouse IL-2, IL-4, and IFN- γ ELISA Kits were purchased from Endogen, Inc. (Woburn, Massachusetts). Lipofectin[®] was purchased from GibcoBRL Life Technologies (Gaithersburg, Maryland). Dioleoyl Phosphatidylethanolamine (DOPE) was from Avanti Polar Lipids, Inc. (Alabaster, Alabama).

Engineering of Cationic Nanoparticles from Microemulsion Precursors

Microemulsion precursors and cationic nanoparticles were engineered as described previously (15). Briefly, emulsifying wax (2 mg) was accurately weighed into 7-mL glass scintillation vials and melted on a hot plate at 50–55°C. Required volumes of deionized and filtered (0.22 μ m) water were added to the melted wax while stirring to form homogeneous milky slurries. Various volumes of a CTAB stock solution (50 mM, in water) were added while stirring to obtain final CTAB concentrations from 5 mM to 30 mM. Within seconds, clear oil-in-water (O/W) microemulsions formed. The droplet size of the microemulsion was measured at 55°C using a Coulter N4 Plus Sub-Micron Particle Sizer (Coulter Corporation, Miami, Florida) at 90-degree light scattering for 90 s. These microemulsions were then simply cooled down (cured) to room temperature while stirring to form nanoparticles. For particle sizing, the nanoparticle suspension was diluted 10-fold with deionized and filtered (0.22 μ m) water and the particle size was measured at 90-degree light scattering for 90 s at 25°C. The zeta potentials of engineered nanoparticles were also measured using a Zeta Sizer 2000 from Malvern Instruments, Inc. (Southborough, Massachusetts).

Stability of Engineered Cationic Nanoparticles in Aqueous and Isotonic Vehicles

Cured nanoparticle suspensions were diluted 10-fold with water, sealed, and stored at room temperature over 6 days. The particle size was measured each day for 6 days as described above. To identify a suitable vehicle for injection, cured nanoparticle suspensions were also diluted 10-fold with either 10% lactose, 10 mM PBS (pH 7.4), or 150 mM NaCl, and the particle size was measured over 30 min at 37°C.

Purification of Engineered Cationic Nanoparticles

To separate free CTAB from the nanoparticles, gel permeation chromatography (GPC) using Sephadex G-75 was performed. Sephadex G-75 was pre-soaked with de-ionized

and filtered (0.22 μ m) water overnight and then packed in a 14 \times 230 mm plastic column. The column was equilibrated with 10% w/v lactose. Five hundred microliters of the cured nanoparticle suspension was applied to the column, and the eluent was collected in 1-mL fractions in plastic vials. The collected fractions were then analyzed by laser light scattering using the N4 Plus Sub-Micron Particle Sizer to identify the fraction containing nanoparticles. In all cases, the seventh fraction contained greatest number of nanoparticles, as evidenced by laser light scattering and zeta potential measurements.

The Preparation and Stability of pDNA-Coated Nanoparticles

Plasmid DNA (CMV- β -gal or CMV-Luc) was coated on the surface of the GPC purified nanoparticles by gently mixing required amounts of pDNA with nanoparticles in suspension. At least 30 min at room temperature was allowed for complete adsorption of pDNA to the surface of the nanoparticles before particle sizing and zeta potential measurements were performed. Net negatively charged pDNA-coated nanoparticles were obtained by coating pDNA on the surface of nanoparticles prepared from emulsifying wax (2 mg/mL) and CTAB (15 mM) to obtain a final pDNA concentration of 75 μ g/mL. The physical stability of pDNA-coated nanoparticles was assessed over 30 min at 37°C by “challenging” pDNA-coated nanoparticles with 150 mM NaCl, 10% fetal bovine serum (FBS) in 150 mM NaCl, or 10% lactose. For particle size measurements, 100 μ L of pDNA-coated nanoparticles was diluted with 900 μ L of the media, and the particle size was measured at 37°C immediately after dilution (0 min) and after 30 min.

The incorporation of DOPE (5% w/w) into the nanoparticles was accomplished by mixing the DOPE with emulsifying wax before microemulsion preparation (15). Cell-specific ligands, cholesterol-mannan and cholesterol-pullulan, were also deposited on the surface of the nanoparticles. Verification of the deposition of cholesterol-mannan was completed by a simple *in vitro* ConA agglutination assay as previously described (15), and that of the cholesterol-pullulan was completed by *in vitro* cell transfection described below. Briefly, each ligand (250 μ g/mL) was mixed with nanoparticles (2 mg/mL) at room temperature under stirring overnight. ConA agglutination assay with GPC-purified mannan-coated nanoparticles demonstrated that 50% (125 μ g) of the cholesterol-mannan ligand was associated with the nanoparticles. Nanoparticles with an endosomolytic lipid (DOPE) and/or the cell-specific ligands (cholesterol-mannan or cholesterol-pullulan) were purified by GPC and pDNA was coated on their surface as described above for cell transfection and immunization studies in mice.

Transmission Electron Micrographs (TEMs)

The size and morphology of nanoparticles were observed using TEM (Philips Tecnai 12 Transmission Electron Microscope) in the Electron Microscopy & Imaging Facility at the University of Kentucky Medical Center. A carbon-coated 200-mesh copper specimen grid (Ted Pella, Inc., Redding, California) was glow-discharged for 1.5 min. Nanoparticle

suspension deposition on the grid and uranyl acetate staining was completed as described previously (16).

In Vitro Transfection of Hep G2 Cells

Hep G2 cells were from American Type Culture Collection (ATCC, Rockville, Maryland) and were maintained in Eagle's Minimum Essential Medium (EMEM; Gibco, BRL) media containing 10% FBS and 1% penicillin-streptomycin (Gibco, BRL). Transfections were performed with cells that were approximately 80% confluent. Cells were plated in 48-well plates at a cell density of 5×10^5 cells/well and incubated overnight. The cells were incubated further with the formulations having a plasmid dose of 2.5 $\mu\text{g}/\text{well}$ and were harvested after 52 h by removing the media, washing with 1X PBS buffer, and then adding 200 μL 1X Lysis buffer (Promega, Madison, Wisconsin) for 5–10 min before freeze-thawing three times. Luciferase activity was assayed as described previously (14). Net positively charged pDNA-nanoparticles (prepared with 6 mg/mL of emulsifying wax and 15 mM CTAB) were used for all cell transfection studies because previous studies showed that net negatively charged pDNA-nanoparticles did not transfect well *in vitro* (15). The pDNA-coated nanoparticles (N) had particle size and zeta potential of 220 ± 5 nm and 44 ± 2 mV, respectively. The particle size and zeta potential of other modified pDNA-coated nanoparticles (with either DOPE or cell-targeting ligands) were comparable (i.e., particle sizes ranged from 205–225 nm, and zeta potentials ranged from +40–44 mV). Statistical analysis was completed using a two-sample *t* test assuming unequal variances. A *P* value < 0.05 was considered to be statistically significant.

Mouse Immunization Studies

Ten- to 12-week-old female mice (Balb/C) from Harlan Sprague-Dawley Laboratories were used for all animal studies. National Institutes of Health guidelines for the care and use of laboratory animals were observed. Mice ($n = 5/\text{group}$) were immunized with either "naked" pDNA or pDNA-coated nanoparticles subcutaneously on day 0, day 7, and day 14 with 5 μg of pDNA. Mice were anesthetized using pentobarbital (i.p.) before each immunization. One-hundred microliters of each formulation was injected on one site on the back. "Naked" pDNA was injected in 150 mM NaCl and pDNA-coated nanoparticles were administered in 10% lactose. On day 28, the mice were anesthetized and bled by cardiac puncture. Sera were separated and stored as described previously (14). Spleens from all naive and immunized mice were also removed, pooled for each group, and processed as described previously (15). β -galactosidase-specific serum IgG titer was quantified by ELISA (14). Splenocyte preparation and cytokine release were performed as described previously (15). Briefly, isolated splenocytes ($5 \times 10^6/\text{well}$) with three replicates were stimulated with β -galactosidase protein (3.3 $\mu\text{g}/\text{well}$) for 60 h at 37°C. Cytokine release was quantified using ELISA kits from Endogen. Statistical analysis was completed using a two-sample *t* test assuming unequal variances. A *P* value < 0.05 was considered to be statistically significant.

RESULTS

Engineering of Cationic Nanoparticles from Microemulsion Precursors

Cationic nanoparticles were engineered directly from O/W microemulsion precursors in a single vial, one-step process. When the required volume of CTAB (50 mM in water) was added into the homogenous milky slurry of melted emulsifying wax in water at 50–55°C, the suspension turned clear within seconds if the final CTAB concentration was over 10 mM. For samples having a final CTAB concentration of ≤ 5 mM, the turbidity of the samples decreased but did not turn clear even after prolonged stirring at 55°C. For all samples, the microemulsion droplet sizes at 55°C were in the range of 30–70 nm, as shown in Fig. 1. Systems made without CTAB were not sized because O/W microemulsions were not formed and the emulsifying wax precipitates were greater than the upper limit of the particle size (i.e., >3 microns). By simple cooling of the O/W microemulsions to room temperature while stirring, cationic nanoparticles were formed having diameters <100 nm when the final CTAB concentration was ≥ 10 mM. In general, the diameters of cured cationic nanoparticles were 12–105% larger than the corresponding microemulsion droplet size and most often about 50% larger.

Stability of the Cured Nanoparticles in Aqueous and Isotonic Vehicles

The final CTAB concentration used to form the microemulsion precursor had a large effect on the stability of cured cationic nanoparticles in water. Cationic emulsifying wax nanoparticles (2 mg/mL) engineered with final CTAB concentrations ranging from 5–30 mM were diluted 1:10 v/v with water, sealed, and stored at room temperature over 6 days. The particle size of cured nanoparticles, made with a final CTAB concentration of either 5 mM or 30 mM, increased by more than 60% from day 1 to day 6 (Fig. 2A). However, the

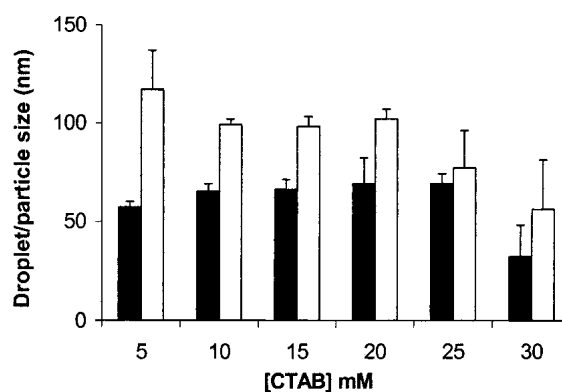


Fig. 1. The preparation of cationic emulsifying wax nanoparticles (2 mg/mL) from microemulsion precursors using CTAB as the cationic surfactant. The microemulsion droplet size at 55°C (black bars) and the cured nanoparticle size at 25°C (white bars) were shown as a function of the final CTAB concentration. One-milliliter microemulsion precursors were prepared at 55°C with emulsifying wax (2 mg/mL) in water using CTAB (5–30 mM) as the surfactant. Emulsifying wax nanoparticles were engineered by simple cooling of the microemulsion precursor. The data reported for droplet size and nanoparticle size are the mean \pm standard deviation for three replicates.

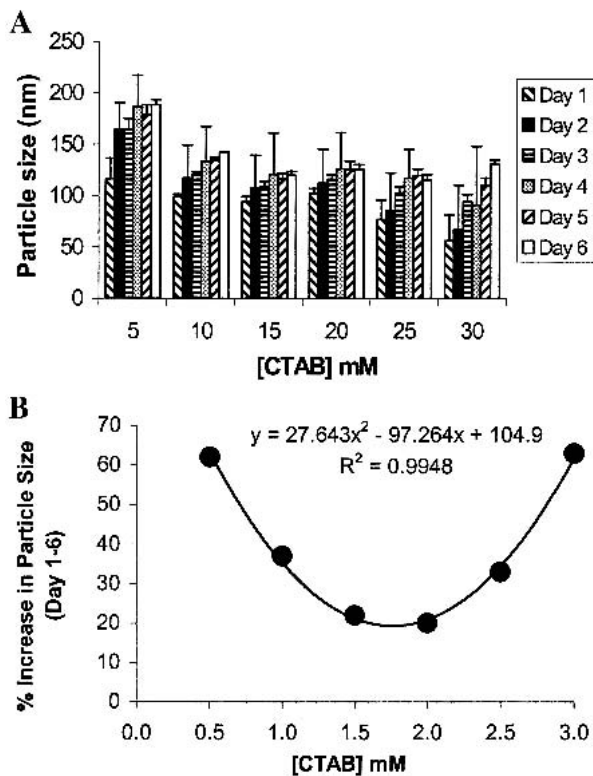


Fig. 2. (A) The stability of cationic emulsifying wax nanoparticles (2 mg/mL) in aqueous suspension stored at room temperature over 6 days. The nanoparticles were engineered as described in Fig. 1. For particle size measurements, 100 μ L of each sample was diluted with 900 μ L of water. (B) The percent increase in cured nanoparticle size from day 1 to day 6 as a function of final CTAB concentration in the O/W microemulsion precursors used to engineer the nanoparticles. Cured nanoparticle suspensions were diluted 10-fold with deionized and filtered (0.22 μ m) water in order to maintain the total light scattering intensity (in counts per second, cps) in the required range of the N4 Plus Sub-Micron Particle Sizer (5×10^4 to 1×10^6 cps). Diluted samples were kept sealed from air in polystyrene cuvettes and stored at room temperature. The data were fitted to a second order polynomial.

particle size of cured nanoparticles made with final CTAB concentrations of 15–20 mM increased by only 20%. As shown in Fig. 2B, there was a strong correlation between the percent increase in cured nanoparticle size from day 1 to day 6 and the final CTAB concentration in the O/W microemulsion precursors used to engineer the cationic nanoparticles. The correlation was a second-order polynomial with an R^2 value of 0.9948. To identify a suitable vehicle for injection, the stability of cationic nanoparticles (2 mg/mL) in three different vehicles was investigated at 37°C over 30 min. There was no change in particle size of the nanoparticles in 10% lactose, 10 mM PBS, pH 7.4, or 150 mM NaCl at 37°C over 30 min (data not shown).

Purification of Nanoparticles

Free CTAB, if any, may cause agglomeration of cured nanoparticles over time. Furthermore, free CTAB in the nanoparticle preparations may interfere with the ability to

efficiently coat nanoparticles with pDNA by the formation of complex or micelle aggregates. CTAB has a critical micelle concentration of 1 mM in water. Thus, free CTAB was removed by GPC (Sephadex G-75) using 10% lactose as the mobile phase. It was confirmed that free CTAB could be easily removed from cationic nanoparticles using GPC with no significant effect on cationic nanoparticle size. As expected, after removing free CTAB, the overall zeta potentials decreased from +60–65 mV to +50–55 mV.

The Stability of pDNA-Coated Nanoparticles in Biologic Milieu

Cationic nanoparticles were engineered as described above, purified to remove free CTAB if any, and sterile filtered through a 0.22- μ m filter before pDNA coating. To prepare net negatively charged pDNA-coated nanoparticles, pDNA was added to a suspension of cationic emulsifying wax nanoparticles (2 mg/mL) so that the final pDNA concentration was 75 μ g/mL. The particle size and zeta potential of net negatively charged pDNA-coated nanoparticles in water was 223 ± 37 nm and -22 ± 1 mV, respectively. Coating the nanoparticles with pDNA increased the particle size by a factor of about 2 to 2.5-fold. GPC of the pDNA-nanoparticles confirmed the association of pDNA with the nanoparticles (data not shown). The results of the stability study, as shown in Fig. 3, demonstrated that the nanoparticles with pDNA were stable over 30 min at 37°C in normal saline, 10% FBS/150 mM NaCl, and 10% lactose.

TEM

Figure 4A shows a typical TEM micrograph of the unpurified nanoparticles engineered using emulsifying wax (2 mg/mL) and CTAB (15 mM). As expected, the nanoparticles were spherical and their size determined by TEM agreed well with that measured by laser light scattering using Photon Correlation Spectroscopy (~ 100 nm). Figure 4B is a TEM micrograph of the pDNA-coated nanoparticles. In contrast to the

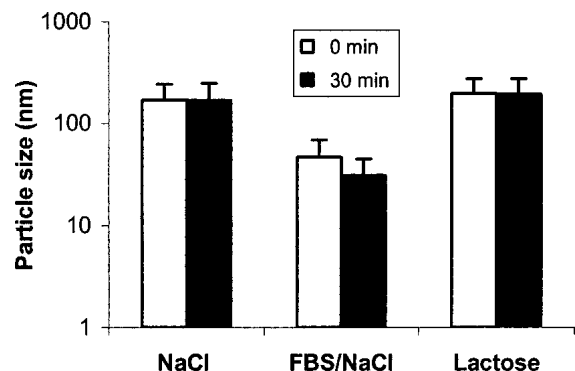


Fig. 3. The particle size of the pDNA-coated nanoparticles (net negatively charged) in various media at 37°C immediately after dilution (0 min) and after 30 min. Plasmid DNA was added to a suspension of GPC purified and filter-sterilized cationic emulsifying wax nanoparticles so that the final pDNA concentration was 75 μ g/mL and the final zeta potential of the pDNA-coated nanoparticles was -22 ± 1 mV. For particle size measurements, 100 μ L of each sample was diluted with 900 μ L of 150 mM NaCl, 10% FBS/150 mM NaCl, or 10% lactose.

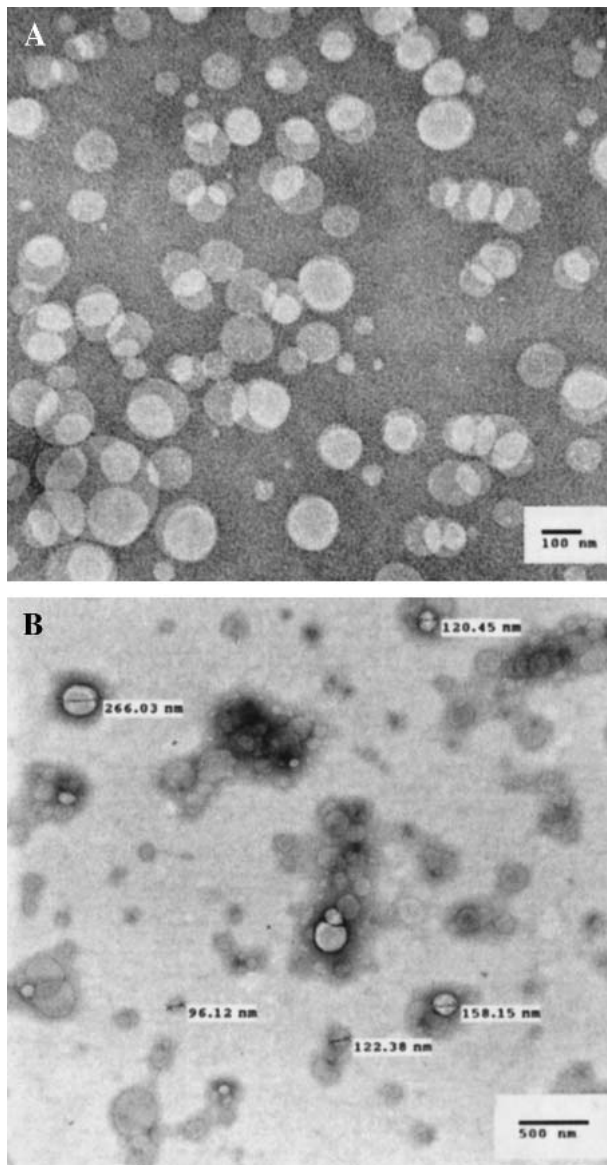


Fig. 4. TEM of the nanoparticles. (A) TEM of unpurified nanoparticles. The nanoparticles were prepared with emulsifying wax (2 mg/mL) and CTAB (15 mM) as in Fig. 1. (B) TEM of purified, pDNA-coated nanoparticles. The nanoparticles in (A) were purified by GPC, and pDNA was coated on their surface to obtain a final pDNA concentration of 75 $\mu\text{g}/\text{mL}$ and final zeta potential of -22 ± 1 mV.

nanoparticles alone (Fig. 4A), some of the nanoparticles coated with pDNA in the micrograph (Fig. 4B) were associated with one another.

In Vitro Transfection of Hep G2 Cells

Commercially available dendritic cells (DC cells) from BioWhittaker were transfected in culture with the pDNA-coated nanoparticles without success (data not shown). Even Lipofectin[®], a commercially available cell transfection reagent, did not result in significant levels of transfection. Therefore, a Hep G2 cell line was chosen to investigate the *in vitro* transfection ability of the pDNA-coated nanoparticles with or without cell-targeting ligands or/and endosomolytic

lipid. Hep G2 cell is an ideal cell line to demonstrate cell targeting with pullulan-coated nanoparticles because it has been reported previously that pullulan can act as a liver targeting ligand *in vivo* (17). Further, pullulan has been used to target antigens and liposomes and nanoparticles containing antigens to immune cells, resulting in enhanced humoral and cellular immune responses (18–20). Figure 5 shows that coating of pDNA on the surface of the cationic nanoparticles significantly enhanced the *in vitro* cell transfection compared to that of “naked” pDNA. As expected, the incorporation of DOPE, an endosomolytic lipid, increased the transfection ability of the nanoparticles by over 5-fold (N + D vs. N) ($P = 0.008$). Surface coating of a Hep G2 cell-targeting ligand, pullulan, a polysaccharide of glucose, increased the transfection ability of the pDNA-coated nanoparticles by over 40-fold (PN vs. N; $P = 0.03$) to levels that were comparable to that of the Lipofectin[®] (Fig. 5). The enhanced cell transfection ability of the pDNA-coated nanoparticles with pullulan can be at least partially attributed to receptor-mediated endocytosis since pre-incubation of the Hep G2 cells with free cholesterol-pullulan for 30 min significantly reduced the transfection efficiency of the pullulan-coated pDNA-nanoparticles, in proportion to the amount of the free cholesterol-pullulan added.

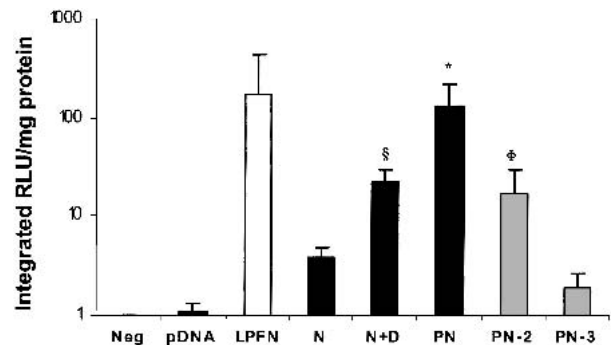


Fig. 5. *In vitro* transfection of liver HepG2 cells (50,000 cells) ($n = 3$) in the presence of 10% FBS after 52 h with: pDNA, Lipofectin[®] (LPFN), nanoparticles (N) with 5% (w/w) DOPE (N + D), and pullulan-coated nanoparticles (PN). For PN-2 and PN-3, 50 μg and 250 μg free cholesterol-pullulan was added 30 min before pullulan-coated nanoparticles to block the glucose receptors. The pDNA dose was 2.5 μg for all samples. As recommended by Dynatech, luciferase expression data were reported as the ratio of the full integral of the samples to that of the negative control (Neg) divided by the total amount of protein in the 20 μL of samples assayed. As mentioned in the Materials and Methods section, the pDNA-coated nanoparticles used for cell transfection study were net positively charged and prepared with emulsifying wax (6 mg/mL) and CTAB (15 mM) (15). The pDNA-coated nanoparticles (N) had particle size and zeta potential of 220 ± 5 nm and 44 ± 2 mV, respectively. The particle size and zeta potential of other modified pDNA-coated nanoparticles (with either DOPE or cell-targeting ligands) were comparable (i.e., particle sizes ranged from 205–225 nm, and zeta potentials ranged from 40–44 mV). *Indicates that the result of PN is significantly different from that of N, N+D, PN-2, and PN-3. §Indicates that the result of N + D is significantly different from that of N. ΦIndicates that the result of PN-2 is significantly different from that of PN-3. In addition, the result of pDNA alone is significantly lower than that of all other groups, except the negative control. Statistical analysis was completed using a two-sample *t* test assuming unequal variances. A result of $P < 0.05$ was considered statistically significant.

Immune Responses after Subcutaneous Administration

As shown in Fig. 6, the total antigen specific IgG titer in serum of mice immunized with pDNA-nanoparticles was enhanced by 3-fold over that of “naked” pDNA, although the result was not statistically significant. Surface deposition of mannan, a DC-targeting ligand, enhanced the immune response by 10-fold over that of “naked” pDNA. Again, this enhancement was not statistically significant ($P = 0.065$) because one of the five mice in the nanoparticle group (group 2, Fig. 6) was a very low responder. Interestingly, a combination of both DOPE and cholesterol-mannan on the pDNA-nanoparticles (group 3, Fig. 6) enhanced the IgG titer by more than 16-fold over that of “naked” pDNA (group 4, Fig. 6; $P = 0.005$).

In vitro cytokine release from isolated splenocytes (5×10^6 /well) after stimulation with β -galactosidase ($3.3 \mu\text{g}/\text{well}$) was also investigated to further characterize the breadth of the immune responses. Immunization with pDNA-coated nanoparticles resulted in a strong Th1-biased cytokine release (Table I) as demonstrated by the significant increase (up to 300%) of Th1-type cytokines IL-2 and IFN- γ . As expected, “Alum”-adjuvanted β -galactosidase protein resulted in very low levels of IL-2 and IFN- γ . The incorporation of DOPE in the nanoparticles as well as the coating of the nanoparticles with mannan significantly enhanced Th1-type cytokine release over that of the DOPE-free and mannan-free nanoparticles. In contrast, “Alum”-adjuvanted β -galactosidase protein resulted in high levels of IL-4 release, whereas all nanoparticle groups and “naked” pDNA resulted in significantly lower, although still positive, IL-4 release.

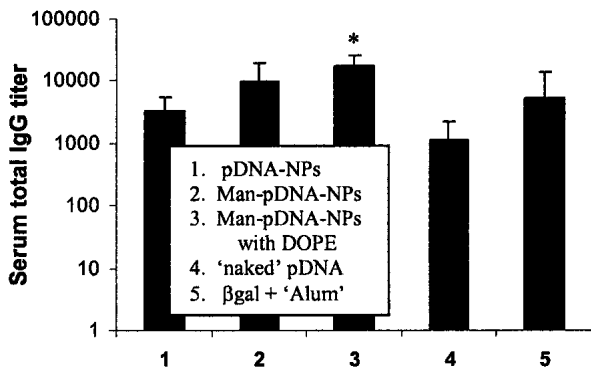


Fig. 6. Antigen-specific total IgG titer in serum to expressed β -galactosidase 28 days after subcutaneous administration. One-hundred microliters containing $5 \mu\text{g}$ of pDNA was administered to anesthetized Balb/C mice on day 0, day 7, and day 14. Plasmid DNA was added to a suspension of cationic emulsifying wax nanoparticles ($2 \text{ mg}/\text{mL}$) so that the final pDNA concentration was $75 \mu\text{g}/\text{mL}$. The particle size and zeta-potential of these nanoparticles (group 1) was $245 \pm 25 \text{ nm}$ and $-42 \pm 1 \text{ mV}$, respectively. The size and zeta potential of other modified nanoparticles (group 2 and 3) were comparable. Groups: (1) pDNA-coated nanoparticles; (2) mannan-coated pDNA-nanoparticles; (3) mannan-coated pDNA-nanoparticles with DOPE (5% w/w); (4) “naked” pDNA. (5) $10 \mu\text{g}$ of β -galactosidase protein adjuvanted with $15 \mu\text{g}$ “Alum”. The data reported are the mean \pm standard deviation of $n = 5$ mice/group. * Indicates that the IgG titer of group 3 is significantly different from that of the group 1, 4, and 5. Statistical analysis was completed using a two-sample *t* test assuming unequal variances. A result of $P < 0.05$ was considered statistically significant.

DISCUSSION

Positive results with the delivery of (genetic) vaccines and *ex vivo* loading of DCs with antigen has strengthened the movement towards directly targeting antigen presenting cells as a means to amplify, control, and mediate the immunologic consequences of prophylactic and/or therapeutic vaccines (2–4). Of particular interest is targeting antigens to the lymph nodes via the skin or subcutaneous routes wherein a rich population of DCs are located (21,22). Moreover, specifically targeting dendritic cells in the skin (Langerhan’s cells) or draining lymph node would theoretically have advantages in eliciting stronger T cell-mediated immunity. The work by Singh *et al.* using pDNA coated on PLGA microspheres demonstrated an enhancement in immune responses using smaller microspheres ($300 \text{ nm} > 1 \mu\text{m} > 30 \mu\text{m}$), which was attributed to the ability of the smaller particles to be taken up by antigen-presenting cells (12). Thus, it was hypothesized that even smaller and more readily engineered nanoparticles may preferentially target antigen-presenting cells, such as DCs, in the skin and draining lymph nodes.

It was demonstrated in this current study that stable cationic nanoparticles having diameters around 100 nm could be engineered from O/W microemulsion precursors formed at increased temperatures (i.e., $40\text{--}55^\circ\text{C}$) and then simply cooled to form stable nanoparticles. Nonionic emulsifying wax (composed of cetyl alcohol and polysorbate 60 in a molar ratio of about 20:1) was selected as the oil phase since it is an approved material and has a melting point of $\sim 50^\circ\text{C}$. The wax is typically used in cosmetics and topical pharmaceutical formulations and is generally regarded as a nontoxic and nonirritant material. For example, cetyl alcohol is currently used as an excipient in the marketed product Exosurf Neonatal[®]. In addition, polysorbate 60 is used in many pharmaceutical products including parenteral products. In these present and previous studies using the engineered nanoparticles, no gross inflammatory, allergic, or toxic effects have been observed in mice after administration of these nanoparticles by the subcutaneous, intramuscular, and topical routes (15).

Microemulsion precursors were engineered using CTAB as the cationic surfactant. Although additional insight is still needed into the relative concentration of CTAB associated with the particles or free in solution, the stability studies of nanoparticles demonstrated both the function and the effect of CTAB in engineering smaller nanoparticles and their resulting stability in suspension over time. Ideally, the system can be optimized so that nanoparticles may be engineered with the most appropriate concentration of CTAB providing small and stable nanoparticles and having only trace amounts of free CTAB. This optimization could lead to an engineering process that avoids the necessity of removing CTAB by GPC, although it was shown that the GPC process had no effect on nanoparticle size. In these present studies, we used net negatively charged pDNA nanoparticles to dose mice because previous studies have shown that net negatively charged nanoparticles elicited stronger immune response than net positively charged nanoparticles (15).

Although the final pDNA concentration was adjusted to $75 \mu\text{g}/\text{mL}$ in this study, the pDNA concentration can easily be increased to $400 \mu\text{g}/\text{mL}$ or even greater by adjusting the amount of the emulsifying wax used to prepare the nanoparticles (15). TEMs showed that the nanoparticles engineered

Table I. *In Vitro* Cytokine Release from Isolated Splenocytes

	Th1 type		Th2 type
	IL-2 (pg/mL)	IFN- γ (pg/mL)	IL-4 (pg/mL)
Naive	546 \pm 54	570 \pm 28	<1
pDNA-NPs	2300 \pm 167	15,098 \pm 360	8.6 \pm 2.4
Mannan-pDNA-NPs	4540 \pm 346 ^b	24,902 \pm 1619 ^c	25.4 \pm 5.5 ^e
Mannan-pDNA-NPs with DOPE	4044 \pm 479 ^b	28,006 \pm 1597 ^{c,d}	57.7 \pm 4.3 ^{e,f}
naked pDNA	1761 \pm 164 ^a	19,971 \pm 393	54.4 \pm 4.5 ^{e,f}
β -gal + "Alum"	171 \pm 13	678 \pm 80	164.4 \pm 14.5 ^g

Note: *In vitro* cytokine release from isolated splenocytes (5×10^6 cells) exposed to β -galactosidase protein for 60 h. Mice were immunized with 5 μ g pDNA or 10 μ g β -Gal (with 15 μ g "Alum") on days 0, 7, and 14 by subcutaneous injection. On day 28, the spleens were removed and pooled for each group. Isolated splenocytes (5×10^6 /well) with three replicates were stimulated with β -galactosidase protein (3.3 μ g/well) for 60 h at 37°C. Cytokine release was quantified using ELISA kits (Endogen).

^a $P < 0.05$ over all nanoparticle groups.

^b $P < 0.05$ over pDNA-NPs.

^c $P < 0.05$ over pDNA-NPs.

^d $P < 0.05$ over Mannan-pDNA-NPs.

^e $P < 0.05$ over pDNA-NPs.

^f $P < 0.05$ over Mannan-pDNA-NPs.

^g $P < 0.05$ over all other groups.

Note: The reported data are the mean \pm standard deviation. Statistical analysis was completed using a two sample *t* test assuming unequal variances. A result of $P < 0.05$ was considered statistically significant.

from O/W microemulsions were spherical having a diameter around 100 nm. Thus, the TEM results agreed well with the results obtained from laser light scattering using photon correlation spectroscopy. Interestingly, when pDNA was coated on the nanoparticles, the surface of the nanoparticles showed an apparent change (Fig. 4B). In contrast to nanoparticles without pDNA, some pDNA-coated nanoparticles appeared to be cross-linked or agglomerated with one another (Fig. 4B). This may be due to the ionic interaction of one pDNA molecule with multiple cationic nanoparticles.

It was shown using Hep G2 cells that the transfection efficiency of pDNA-coated nanoparticles could be enhanced 5- to 10-fold by the inclusion of DOPE (Fig. 5). DOPE had been shown to enhance the transfection efficiency of cationic liposomes, possibly due to disruption of the endosomal membrane (23,24). Further, the inclusion of pullulan as a ligand for hepatocyte specific targeting on the surface of the pDNA-coated nanoparticles was shown to enhance the transfection efficiency by 40-fold to levels that were comparable to that of the reagent, Lipofectin[®]. As a whole, these results demonstrated the potential versatility of these nanoparticles in that both endosomolytic lipids and cell-targeting ligands could be incorporated into this system.

Mouse and human DCs have been shown to express a mannose-receptor, and this receptor has been exploited to deliver antigens resulting in more robust Th1 and CTL responses (25–28). It was demonstrated in this present study that a hydrophobized mannan derivative (cholesterol-mannan) coated on the surface of these nanoparticles resulted in a further enhancement of total IgG titer (Fig. 6) and both Th1-type and Th2-type cytokine release (Table I). More interestingly, a combination of an endosomolytic lipid (DOPE) and the mannan-ligand on the pDNA-coated nanoparticles significantly enhanced serum antigen-specific IgG titer and Th1-type cytokine release over pDNA alone.

The overall improvement of the mannan-coated nanoparticles over nanoparticles alone was modest as compared to previous studies using mannan-coated liposomes (28). However, our studies investigated only one concentration of mannan coating and only one route of administration. Additional studies investigating alternative concentrations and routes (i.e., topical or intradermal) are currently underway. Further, alternative ligands having even greater affinity for DCs (such as peptides derived from phage display) may be of further interest for coating on the surface of these nanoparticles for immunization.

ACKNOWLEDGMENTS

This work was supported, in part, by NSF Grant BES-9986441, and from the AFPE and the Burroughs Wellcome Fund through the AACP New Investigators Program for Pharmacy Faculty. We would also like to thank Mr. Marvin Ruffner in the laboratory of Dr. Jerry Woodward for assistance with the cytokine release assays. Dr. Woodward is in the Department of Microbiology and Immunology at the University of Kentucky Medical Center.

REFERENCES

1. J. B. Ulmer, J. Donnelly, S. E. Parker, G. H. Rhodes, P. L. Felgner, G. H. Rhodes, P. L. Felgner, V. J. Dworki, S. H. Gromkowski, R. R. Deck, C. M. DeWitt, A. Friedman, L. A. Hawe, K. R. Leander, D. Martinez, H. C. Perry, J. W. Shiver, D. L. Montgomery, and M. A. Liu. Heterologous protection against influenza by injection of DNA encoding a viral protein. *Science* **259**:1745–1749 (1993).
2. D. Tang, M. DeVit, and S. A. Johnston. Genetic immunization is a simple method for eliciting an immune response. *Nature* **356**: 152–154 (1992).
3. M. A. Liu, M. R. Hilleman, and R. Kurth (eds.), *DNA Vaccines: A New Era in Vaccinology*, Vol. 772, Ann. NY Acad Sci., New York, 1995.

4. J. B. Ulmer, J. C. Sadoff, and M. A. Liu. DNA vaccines. *Curr. Opin. Immunol.* **8**:531–536 (1996).
5. M. A. Liu. The immunologist's grail: Vaccines that generate cellular immunity. *Proc. Natl. Acad. Sci. USA* **94**:10496–10498 (1997).
6. M. A. Barry and S. A. Johnston. Biologic features of genetic immunization. *Vaccine* **15**:788–791 (1997).
7. H. L. Robinson and C. T. Torres. DNA vaccines. *Semin. Immunol.* **9**:271–283 (1997).
8. M. J. Roy, M. S. Wu, L. J. Fuller, L. G. Tussey, S. Speller, J. Culp, J. K. Burkholder, W. F. Swain, R. M. Dixon, G. Widera, R. Vessey, A. King, G. Ogg, A. Gallimore, J. R. Haynes, and D. Heydenburg Fuller. Induction of antigen-specific CD8+ cells, T helper cells, and protective levels of antibodies in humans by particle-mediated administration of a hepatitis B virus DNA vaccine. *Vaccine* **19**:764–778 (2000).
9. M. A. Conway, L. Madrigal-Estebas, S. McClean, D. J. Brayden, and K. H. Mills. Protection against *Bordetella pertussis* infection following parenteral or oral immunization with antigens entrapped in biodegradable particles: effect of formulation and route of immunization on induction of Th1 and Th2 cells. *Vaccine* **19**:1940–1950 (2001).
10. M. G. Cusi, R. Zurbriggen, M. Valassina, S. Bianchi, P. Durrer, P. E. Valensin, M. Donati, and R. Gluck. Intranasal immunization with mumps virus DNA vaccine delivered by influenza virosomes elicits mucosal and systemic immunity. *Virology* **277**:111–118 (2000).
11. M. L. Hedley, J. Curley, and R. Urban. Microspheres containing plasmid-encoded antigens elicit cytotoxic T-cell responses. *Nat. Med.* **4**:365–368 (1998).
12. M. Singh, M. Briones, G. Ott, and D. O'Hagan. Cationic microparticles: A potent delivery system for DNA vaccines. *Proc. Natl. Acad. Sci. USA* **97**:811–816 (2000).
13. K. D. Newman, D. L. Sosnowski, G. S. Kwon, and J. Samuel. Delivery of MUC1 mucin peptide by Poly(D,L-lactic-co-glycolic acid) microspheres induces type 1 T helper immune responses. *J. Pharm. Sci.* **87**:1421–1427 (1998).
14. Z. Cui and R. J. Mumper. Chitosan-based nanoparticles for topical genetic immunization. *J. Control. Release* **75**:409–419 (2001).
15. Z. Cui and R. J. Mumper. Topical Immunization using nanoengineered Genetic Vaccines. *J. Control. Release* **81**:173–184 (2002).
16. F. C. MacLaughlin, R. Mumper, J. Wang, J. Tagliaferri, I. Gill, M. Hinchcliffe, and A. P. Rolland. Chitosan and depolymerized chitosan oligomers as condensing carriers for in vivo plasmid delivery. *J. Control. Release* **56**:259–272 (1998).
17. Y. Kaneo, T. Tanaka, T. Nakano, and Y. Tamaguchi. Evidence for receptor-mediated hepatic uptake of pullulan in rats. *J. Control. Release* **70**:365–373 (2001).
18. X. G. Gu, M. Schmitt, A. Hiasa, Y. Nagata, H. Ikeda, Y. Sasaki, K. Akiyoshi, J. Sunamoto, H. Nakamura, K. Kuribayashi, and H. Shiku. A novel hydrophobized polysaccharide/oncoprotein complex vaccine induces in vitro and in vivo cellular and humoral immune responses against HER2-expressing murine sarcomas. *Cancer Res.* **58**:3385–3390 (1998).
19. N. Venkatesan and S. P. Vyas. Polysaccharide coated liposomes for oral immunization—development and characterization. *Int. J. Pharm.* **10**:169–177 (2000).
20. L. Wang, H. Ikeda, Y. Ikuta, M. Schmitt, Y. Miyahara, Y. Takahashi, X. Gu, Y. Nagata, Y. Sasaki, K. Akiyoshi, J. Sunamoto, H. Nakamura, K. Kuribayashi, and H. Shiku. Bone marrow-derived dendritic cells incorporate and process hydrophobized polysaccharide/oncoprotein complex as antigen presenting cells. *Int. J. Oncol.* **14**:695–701 (1999).
21. C. Reis e Sousa, P. D. Stahl, and J. M. Austyn. Phagocytosis of antigens by Langerhans cells in vitro. *J. Exp. Med.* **178**:509–519 (1993).
22. J. M. Austyn. New insights into the mobilization and phagocytic activity of dendritic cells. *J. Exp. Med.* **183**:1287–1292 (1996).
23. H. Farhood, N. Serbina, and L. Huang. The role of dioleoyl phosphatidylethanolamine in cationic liposome mediated gene transfer. *Biochim. Biophys. Acta* **1235**:289–295 (1995).
24. L. Huang, H. Farhood, N. Serbina, A. G. Teepe, and J. Barsoum. Endosomolytic activity of cationic liposomes enhances the delivery of human immunodeficiency virus-1 trans-activator protein (TAT) to mammalian cells. *Biochem. Biophys. Res. Commun.* **217**:761–768 (1995).
25. R. Jordens, A. Thompson, R. Amons, and F. Koning. Human dendritic cells shed a functional, soluble form of the mannose receptor. *Int. Immunol.* **11**:1775–1780 (1999).
26. A. J. Engering, M. Cella, D. Fluitsma, M. Brockhaus, E. M. Hoefsmit, A. Lanzavecchia, and J. Pieters. The mannose receptor functions as a high capacity and broad specificity antigen receptor in human dendritic cells. *Eur. J. Immunol.* **27**:2417–2425 (1997).
27. M. C. Tan, A. M. Mommas, J. W. Drijfhout, R. Jordens, J. J. Onderwater, D. Verwoerd, A. A. Mulder, A. N. van der Heiden, D. Scheidegger, L. C. Oomen, T. H. Ottenhoff, A. Tulp, J. J. Neeffes JJ, and F. Koning. Mannose receptor-mediated uptake of antigens strongly enhances HLA class II-restricted antigen presentation by cultured dendritic cells. *Eur. J. Immunol.* **27**:2426–2435 (1997).
28. S. Toda, N. Ishii, E. Okuda, K. I. Kusakabe, H. Arai, K. Hamajima, I. Gorai, K. Nishioka, and K. Okuda. HIV-1-specific cell-mediated immune responses induced by DNA vaccination were enhanced by mannan-coated liposomes and inhibited by anti-interferon- γ antibody. *Immunology* **92**:111–117 (1997).